

Millimeter-Wave in Milliseconds: Sliding Window Network Coding Outperforms Rateless Codes

Eurico Dias, Duarte Raposo, Homa Esfahanizadeh, Alejandro Cohen, Tânia Ferreira, Miguel Luís, Susana Sargento, and Muriel Médard

Abstract—Ultra-reliability and low-latency are pivotal requirements of the new generation of communication networks. Over the past years, to increase throughput, adaptive active antennas were introduced in advanced wireless communications, specifically in the domain of millimeter-wave (mmWave). Consequently, new lower-layer techniques were proposed to cope with the higher dimensional and electronic steerable beams. The transition from omni-directional to highly directional antennas presents a new type of wireless systems that deliver high bandwidth, but that are susceptible to high losses and high latency variation. Classical approaches cannot close the rising gap between high throughput and low delay in those advanced systems. In this work, we incorporate effective sliding window network coding solutions in mmWave communications. While legacy systems such as rateless codes improve delay, our results show that they do not provide low latency communications (LLC - below 10 ms), but fixed sliding window random linear network coding (RLNC), does. Moreover, adaptive sliding window RLNC obtains ultra-reliable LLC (URLLC - LLC with maximum delay below 10 ms with more than 99% probability).

I. INTRODUCTION

Millimeter-wave (mmWave) networks enable multi-gigabit-per-second data rates between 57 GHz and 64 GHz, the so-called V-Band, that uses the unlicensed spectrum available worldwide. It is an attractive option for Integrated and Access Backhaul (IAB), which is proposed for the new generation of communications - 5G and beyond - to reduce deployment expenses of fiber optics with the introduction of high-density 5G small cells [1]. However, these frequency bands have been heretofore mostly idle because mmWave communications suffer from strong path loss, and heavy propagation challenges with obstacles, rain and atmospheric absorption, making them only suitable for short and line-of-sight (LOS) communications. Recent advances in the use of small antenna arrays, capable of forming highly dimensional and electronically steerable beams, and beamforming techniques like the Sector Level Sweep [2], can partially ameliorate the effects of propagation characteristics [3] but with associated complexity and costs.

The challenges of mmWave are particularly salient when we seek to use them, as would be the case in IAB, for low latency

E. Dias, D. Raposo and T. Ferreira are with Instituto de Telecomunicações, Aveiro, Portugal (e-mail:eurico.omdias, dmraposo, tania.s.ferreira@av.it.pt). H. Esfahanizadeh and M. Médard are with the EECS Department, Massachusetts Institute of Technology (MIT), Cambridge, MA 02139 USA (email: medard, homaesf@mit.edu). A. Cohen is with the Faculty of ECE, Technion, Israel (e-mail: alecohen@technion.ac.il). M. Luís is with Instituto Superior de Engenharia de Lisboa and Instituto de Telecomunicações, Portugal (e-mail:nmal@av.it.pt). S. Sargento is with the University of Aveiro and Instituto de Telecomunicações, Portugal (e-mail:susana@ua.pt).

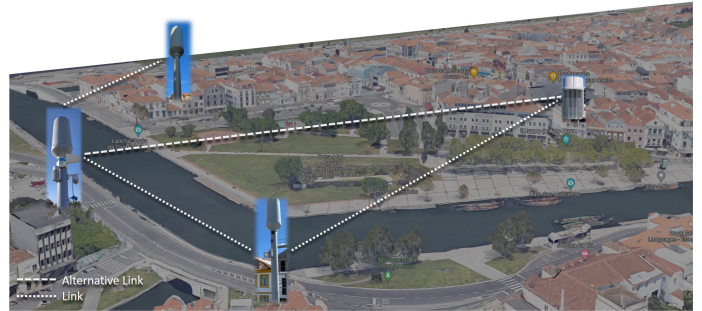


Fig. 1: Aveiro Living Lab mmWave infrastructure (Portugal): Four mmWave antennas are connected with LOS links [16].

communication (LLC: latency below 10 ms) and ultra-reliable LLC (URLLC: LLC with more than 99% success probability). The lossy nature of mmWave introduces new challenges (e.g., link quality assessment, rate adaptation and bufferbloat) in the transport layers [4]. Error-control mechanisms at the transport layer can tackle the dramatic path loss of mmWave communications. Several techniques have been used to correct failures in wireless channels, e.g., rateless erasure codes [5], [6], which were recently deployed [7], systematic codes [8], and streaming codes [9], [10]. In order to manage delay, transport protocols commonly use windowing schemes, such as TCP [11], [12]. Combining windowing with coding can be done with RLNC either in a fixed scheme [13], [14] (F-SW-RLNC) or in an adaptive way [8], [15] (A-SW-RLNC).

Recently, a causal A-SW-RLNC scheme was proposed in [17], [18]. The main idea is to track the channel state to adjust the size of the window of packets used to form the RLNC-coded packet in a causal fashion. This feature adaptively tunes the redundancy ratio and error correction capability of the coding solution. In this paper, we look into the unique dynamic behaviour of mmWave communication environment, and propose how to use SW-RLNC, both as the F-SW-RLNC and as the A-SW-RLNC version of [17], [18], to capture rapid changes and mitigate the high losses that are intrinsic to mmWave, for LLC and URLLC. For our study, we have collected a representative dataset in the mmWave backhaul network deployed in the city of Aveiro (Fig. 1). The obtained results show that A-SW-RLNC scheme could obtain URLLC.

The remaining of this paper is organized as follows: Section II describes the mmWave technology - PHY and MAC layer mechanisms -, the system model and problem formulation. Section III presents different RLNC approaches, and in spe-

cific, the A-SW-RLNC. Section IV presents the experimental network test scenario, the methodology, the impact of modulation coding schemes in the packet loss, and the results of the experiment by comparing the RLNC rateless approaches with A-SW-RLNC in terms of throughput, mean in-order delay, and maximum in-order delay. Finally, section V summarizes the findings and discusses future research directions.

II. PROBLEM STATEMENT

This section provides a technical background of mmWave technology, the system model and the problem formulation.

A. Millimeter Wave Technology

The wireless propagation channel can vary significantly over time, greatly affecting the radio's link quality. This is especially significant for technologies that operate in the mmWave band, such as IEEE 802.11ad [19], as the higher frequencies cause higher susceptibility to the blockage.

To mitigate the negative impact of obstructions, Wigg-based COTS devices, such as the CCS Metnet nodes [20], employ an automatic mode to dynamically select the parameters of modulation and error correction based on the instantaneous signal-to-noise ratio (SNR) and error rate [21]. Specifically, devices can switch between four modes of operation, each having specific modulation and Forward Error Correction (FEC) schemes, and all utilize the 60 GHz carriers: a) control PHY (MCS 0); b) Single carrier (MCS 1-12) PHY; c) OFDM (MCS 13-24) PHY; and d) low-power SC (and MCS 25-31) PHY. This set of choices makes it possible to meet different performance requirements, depending on the usage scenario (e.g., low-interference, low-complexity, low-energy-consumption, etc.). The 802.11ad PHY standard supports Low-Density Parity-Check (LDPC) codes with four different rates (1/2, 5/8, 3/4, and 13/16), with a fixed codeword length of 672 bits [22]. Each modulation type combined with a specific code rate form a Modulation and Coding Scheme (MCS). More details regarding the modulation schemes, code rates and data rates that are supported by each MCS are specified in Table I. For the L2 line rate calculation the manufacturer adopts a maximum frame size of 2000 bytes.

Fig. 2 shows the relevant PHY layer (RCPI, SNR, and PER) and transport layer metrics (packet loss), measured in

TABLE I: Different Modulation and Coding for Single carrier PHY mode supported by the CCS Metnet node [19].

MCS	MOD	FEC rate	Min. Req. RCPI (dBm)	Min. Req. SNR (dB)	Layer 2 Line Rate (Mbps)
0	DSSS	12	-84.52	-11	22.4
1	BPSK	1/2	-73.72	-0.2	308
2	BPSK	1/2	-72.52	1	616
3	BPSK	5/8	-71.32	2.2	770.4
4	BPSK	3/4	-69.92	3.6	924
5	BPSK	13/16	-69.02	4.5	1000.8
6	QPSK	1/2	-69.72	3.8	1232
7	QPSK	5/8	-68.22	5.3	1540
8	QPSK	3/4	-66.72	6.8	1848
9	QPSK	13/16	-65.72	7.9	2002.4

the outdoor testbed described in section IV-A, for different MCS modes (fixed and automatic) in an obstructed scenario. In addition, this figure shows the minimum required levels of SNR and RCPI reported by the manufacturer for maintaining each MCS (the dashed horizontal lines). As shown, under obstruction, the RCPI signal level drops to a lower value than the defined threshold for almost all fixed MCSs (with the exception of MCS 1). However, the SNR requirement is still being fulfilled most of the time. Note that sudden decreases of the RCPI and SNR occurred due to slight obstacle movements. Moreover, the figures show that using higher modulation indexes in an obstructed scenario may lead to packet error rates up to 90% in the PHY layer, and packet loss rate up to 100% in the transport layer. On the other hand, automatic modulation adjustment leads to lower packet losses and packet error rates under a static obstruction.

Still, switching MCS to a more robust scheme (i.e., with a lower code rate) whenever the signal quality drops may not be enough to ensure a reliable connection. This is because a sudden obstruction of the line-of-sight path can cause a significant decrease in the maximum achievable throughput, increasing the delay. This leads to several issues in the upper layers, such as, link quality judgment, rate adaptation, bufferbloat [4], [23]. Link fluctuations will affect TCP performance when mmWave links switch between LOS and NLOS links states, resulting in TCP retransmissions, an increase of the RTT, and consequently the decrease of the congestion window. The variability of the links will also prevent some protocols to achieve the ultra-high bandwidth capacity of the mmWave links. The bandwidth-delay product (BDP) used to compute the optimal buffer size will be difficult to estimate, resulting in high latency and jitter with the use of larger buffers to prevent packet loss. Thus, algorithms that are faster to adapt to the conditions of the link

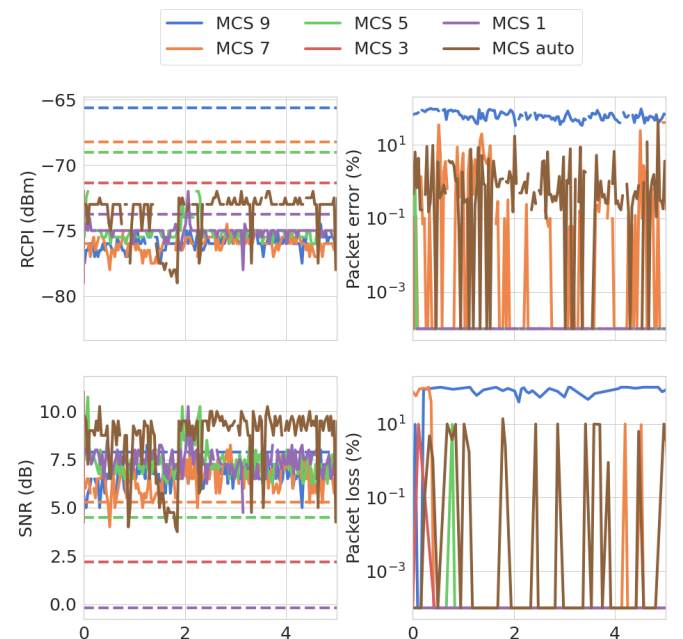


Fig. 2: Measurements for PHY and MAC layer under blockage, for a time interval of 5 minutes.

will have some advantages (e.g., A-SW-RLNC).

In those cases, we use an effective network coding solution that can be introduced in the transport layer to mitigate the losses and handle the high variations of delay caused by obstructions. This, in turn, lightens the requirements of the FEC mechanisms implemented at the PHY layer. This is especially useful in mmWave networks where blockage increases the delay, packet losses, and the number of TCP retransmissions.

B. System Model and Problem Formulation

We consider a real-time slotted mmWave communication with feedback. In particular, a single-path (SP) communication setting is considered between two points, sender and receiver, and we assume that the data that needs to be communicated consists of N packets of the same size, i.e., $\{P_1, \dots, P_N\}$. At the i -th time step, the sender transmits a coded packet E_i over the noisy mmWave forward channel. The receiver may acknowledge the sender by sending an acknowledgment (ACK) for any delivered coded packet over the noisy feedback channel. The delay between the first time data is transmitted and the time that the corresponding feedback is received is called round-trip-time (RTT). The transmission delay of coded packet t_d is the time it takes for the sender to transmit one packet (push the packet into the medium), and the propagation delay t_{prop} is the amount of time it takes for one packet to be received from the sender to the receiver. We assume that the size of the feedback acknowledgment is negligible, and that the propagation delay can vary for any transmitted coded packet according to the channel's condition. Hence, the RTT for each coded packet is equal to $t_d + 2t_{\text{prop}}(E_i)$, where $t_{\text{prop}}(E_i) \leq t_{\text{prop}}$. Let the timeout $t_o \geq 2t_{\text{prop}}$ to denote an adaptive parameter the sender may choose to declare the packets that were not delivered at the receiver. That is, for any coded packet transmitted, if an ACK is not received at the sender after $t_d + t_o$ time slots, the sender declares a negative-acknowledgment (NACK) for the corresponding packet.

Our main performance metrics are defined as follows:

- (1) **Throughput η** . This is defined as the rate, in units of bits per time slot, at which the information is delivered at the receiver. In this paper, we focus on a normalized throughput, denoted by η , which corresponds to the total number of information bits delivered to the receiver divided by the total amount of bits transmitted by the sender.
- (2) **In-order delivery delay of packets D** . This is the difference between the time slot in which an information packet is first transmitted at the sender and the time slot in which the packet is decoded, in order, by the receiver.

Our goal in this setting is to maximize the throughput, while minimizing the in-order delivery delay of packets.

III. NETWORK CODING FOR JOINT SCHEDULING AND CODING

This section elaborates on using RLNC as an error correction mechanism in the transport layer between two points. This mechanism mitigates the rigid requirements of the physical layer error correction code to provide reliable communications

for the worst mmWave channel condition. Thus, one can increase the performance in terms of throughput and delay as defined in Section II-B.

In classical RLNC schemes [13], [14], each encoded packet E_i , where i is a positive integer, that is transmitted over the lossy communication is a random linear combination of the original uncoded packets, i.e.,

$$E_i = \sum_{j=1}^N \rho_{i,j} P_j, \quad (1)$$

where the coefficients $\{\rho_{i,j} : i \in \{1, 2, \dots\}, j \in \{1, \dots, N\}\}$ are drawn from a sufficiently large field, and N is the total number of original uncoded packets. In general, when the coefficients are randomly sampled from a large field, the receiver can decode the original packets once N coded packets are received, for example using the Gaussian elimination technique.

Although classical RLNC schemes can achieve the desired communication rates in the realm of large N , this imposes a large latency to the system, since for decoding the first packet, at least N coded packets need to be transmitted. Thus, some variations of RLNC have been studied in the literature to lower the latency [5], [6], [8]–[10], [17]. In our proposed scheme, we compare part of these methods, which will be next described, over several mmWave settings.

A. Rateless RLNC (R-RLNC)

In this variation, the sender's packets are split into non-overlapping blocks, called batches, each with size of n packets. The batches are encoded and transmitted in order. For each batch, the encoded packets are random linear combinations of the packets within the same batch, and the ratio of the number of original packets n and the number of encoded packets m denotes the rate of the scheme. In a well-designed scheme, the receiver is able to recover the whole batch per receipt of its n out of m encoded packets. More precisely, let E_i^k be the k -th encoded packet of the i -th batch, then

$$E_i^k = \sum_{j=1}^n \rho_{i,j}^k P_{(i-1)n+j}. \quad (2)$$

In this variation, the code designer in advance can try to manage the performance, in terms of throughput and latency trade-off, by choosing the size of n and m .

Recently, there are new solutions in the literature that proposed solutions in which the size of the i -th uncoded batch $n(i)$ and the size of the i -th coded batch $m(i)$ can be time-variant and adapted based on the channel estimation [15], [24]. However, those solutions are only adaptive and reactive to the mean packet loss probability. In mmWave communications, the channel conditions vary extremely fast; hence, although the above solutions are adaptive, one can pay in performance as those solutions do not track the specific erasure pattern of each packet and batch.

B. Adaptive and Casual RLNC

This is an adaptive and casual variant (A-SW-RLNC method), as given in [17]. In this method, at each time a packet is transmitted and according to the feedback information, the sender can decide either to transmit a new coded linear combination, i.e., *new packet*, or repeat the last sent combination, *same packet*. Here, *same* and *new* refer to the raw information packets contained in the linear combination, such that sending the same linear combination means that the raw information packets are the same but with different random coefficients. Thus, using a sliding window mechanism, the i -th coded packet can be described as follows,

$$E_i = \sum_{j=w_{\min}}^{w_{\max}} \rho_{i,j} P_j, \quad (3)$$

where w_{\min} corresponds to the oldest raw information packet that is not yet decoded, and w_{\max} is incremented each time a new raw information packet is decided to be included in the linear combination by the sender.

The A-SW-RLNC solution tracks the channel conditions, and adaptively adjusts the retransmission rates based on the channel quality and the feedback acknowledgments. For the channel estimation, the behavior of the channel parameters (i.e. erasure probability and its variance) is tracked using the feedback acknowledgements over time. A-SW-RLNC envisions two different FEC mechanisms to add redundancy (retransmissions) and coping with the errors and failures, according to the channel status. The first one is *apriori* and the second one is *aposteriori*, and they both interplay to obtain a desired throughput-delay trade-off. The first FEC mechanism is *apriori*, as it sends redundant packets in advance (before the failure occurs) according to the average estimation of the channel behavior. The second FEC mechanism is *aposteriori*, as it sends redundant packets according to the realization of errors, identified using the feedback information. It is through the second mechanism that the sender ensures that decoding is eventually possible at the receiver. We note that the higher number of *apriori* FECs is, the lower is the delay and the throughput, as it pro-actively recovers (possibly more than needed) for future lost coded packets. On the other hand, the

¹Here, it is assumed that the total number of packets is divisible by the block size. If not, one can easily use the zero-padding techniques.

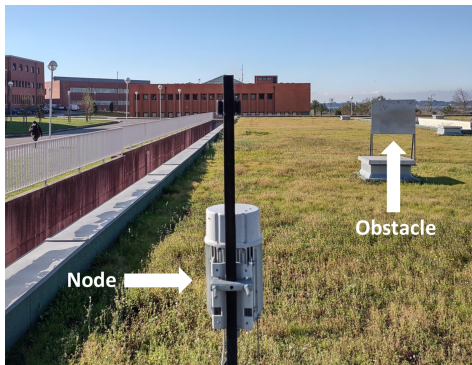


Fig. 3: Blockage scenario with the metal obstacle.

higher the number of *aposteriori* FECs is, the higher is the delay and the throughput, as it only recovers for the needed lost coded packets at the cost of a delay proportional to RTT. The way to adjust this trade-off is through an adaptive approach, which is described in detail in [17].

IV. EXPERIMENTAL STUDY AND PERFORMANCE EVALUATION

This section presents the experimental study and scenarios and discusses the obtained results.

A. Experimental mmWave Network Test Scenario

The mmWave network is composed of three CCS Metnet nodes [20], which are presented in Fig. 4. These nodes were deployed in an outdoor environment, specifically on the rooftop of IT in Aveiro (Portugal), which allowed running tests under a fully controlled environment.

The deployed network adopts an architecture where node PCP, called the Personal Basic Service Set (PBSS) coordinator, has a wired connection to the core network. On the other hand, nodes A and B, the remote nodes, access the network through the radio links they establish with the node PCP. For each node, there is an APU connected, that will communicate using the mmWave backhaul.

Furthermore, these nodes employ the standardized IEEE 802.11ad (WiGig) technology, which operates between the 57 GHz to 66 GHz unlicensed frequencies, to form a wireless 5G meshed backhaul capable of accommodating hundreds of gigabits traffic from the core network. Each device has four radio modules, each employing a 19 dBi beamforming steerable antenna that establishes directional links to cope with the increased attenuation at 60 GHz. For that purpose, the Wigig standard has proposed MAC and PHY layer enhancements which include support for directional communication through a process known as beamforming training, which allows determining the appropriate transmit and receive antenna sectors for communication between a given pair of stations. By employing beamforming techniques, the 300° horizontal field covered by each device is divided into 64 discrete sectors (with a 5° horizontal beamwidth) that can be used to concentrate the signal towards a specific direction.

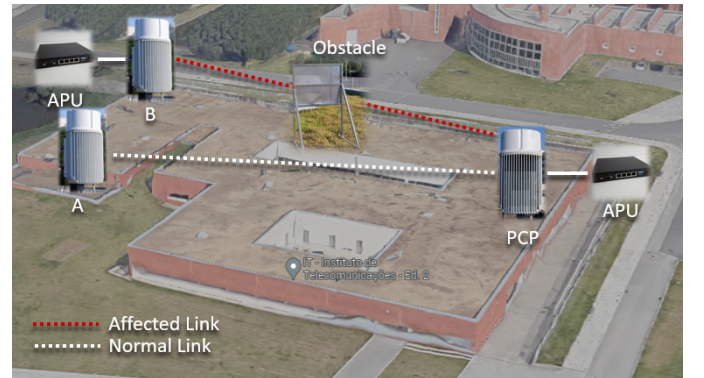


Fig. 4: Experimental mmWave Network Test Scenario.

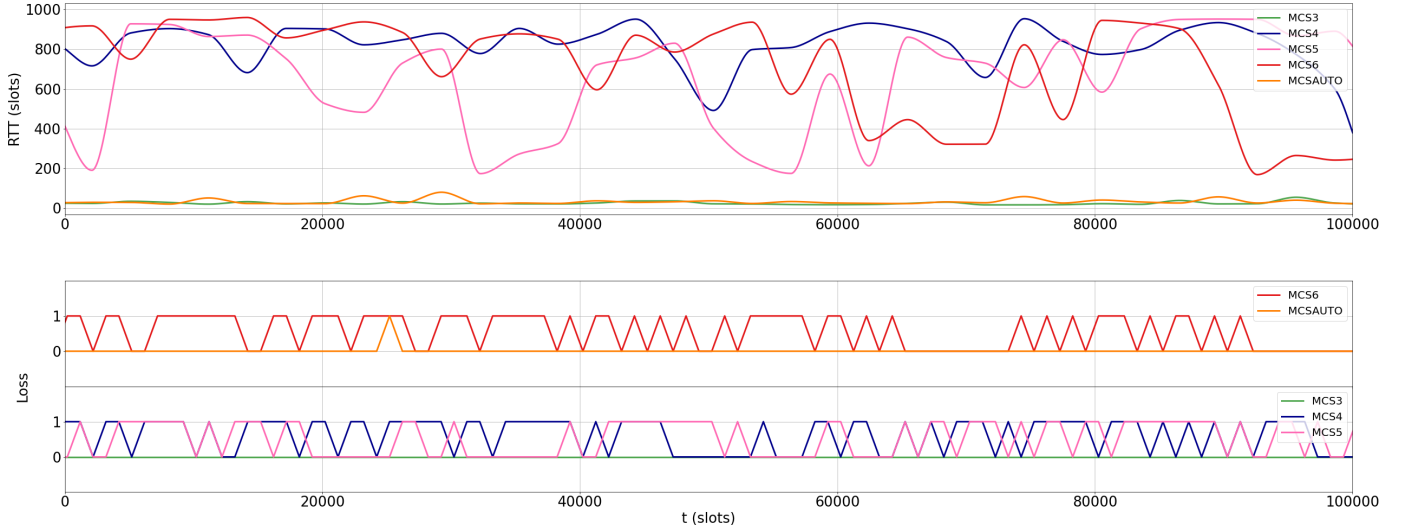


Fig. 5: RTT and Loss pattern collected in the experimental mmWave network (in a blocked scenario with a metal obstacle), using different MCS(3-6) and MCSAuto.

In the experimental scenario, a metallic obstacle was placed between two stations (STAs) to simulate the blockage scenario represented in Fig. 3. This obstacle was maintained in a fixed location for the entire test duration (30 minutes). After the introduction of the obstruction, a significant reduction of the instantaneous RSSI and SNR was observed compared to the average values registered under non-obstructed operation Fig. 2.

B. Methodology

The dataset generation was performed in the available test scenario of the mmWave network, presented in Fig. 3 and Fig. 4. The data collection aims to gather the channel characteristics at each transmission, specifically the RTT and the realizations. Thus, UDP traffic was generated, and at the same time, the round-trip time and the state of the packet were collected using the TWAMP tool. The tool integrates a larger set of network performance measurement tools from PerfTools and implements the Two-Way Active Measurement Protocol (TWAMP), defined in the RFC 5357 [25]. Under the presented scenario, one of the Linux APU nodes was selected to be the sender, while the other was setup to be the reflector. The TWAMP tool was executed as a server on the reflector APU, up until the conclusion of the dataset creation. The raw and unprocessed dataset consists of a 5-minute execution of the TWAMP sender, for each MCS values from MCS3 through MCS6, fixed on the Metnet CCS radio nodes. The generation was also performed on the MCS auto mode. The limitation of the size and time-slot definitions was possible by sending a limited amount of packets, and by setting the interval between transmissions – the chosen value, obtained by trial and error, was the maximum the tool would support without losing packets due to its limitations on the APU, which was $450 \mu\text{s}$. To minimize the error of the measurements, given that TWAMP one-way directional delays are clock sensitive, the system clocks on the APUs were synchronized using the internal university Network Time Protocol (NTP) server,

forced after each periodic measuring process. The datasets were then post-processed using a Python script, to extract losses and per-packet round-trip time vectors.

To test the generated network state vectors against the presented set of algorithms, a RLNC simulator was developed, using Python, through the Steinwurf's Kodo Python library [26]. The implementation code for the encoding and decoding of packets were based on the *Block* and *Slide* RLNC base examples.

The simulator executes the above algorithms for each collected MCS value available on the dataset, and obtains the results of executions - datapoints - along the mmWave network condition vectors. Each successful delivery under the defined scenario over an algorithm is defined as an experience. The completion of an experience outputs a triple, consisting of the normalized throughput, the mean and the maximum in-order delay metrics. A datapoint is then defined as the mean of each metric of 10 triples (i.e., experiences) added with the starting timeslot (i.e., index) on the vector. The simulation will complete when all timeslots from the vector are used (i.e., the length of the vectors is exhausted). The total set of datapoints is then stored per tested MCS and algorithm.

The considered algorithms tested and presented on this paper are the Rateless RLNC (sec. III-A), a Sliding Window variant of the Rateless RLNC (F-SW-RLNC), and finally the A-SW-RLNC implementation (sec. III-B). The above algorithms were implemented and tested using each pair of vectors. The baseline scenario is represented as a UDP transmission of a pseudo-randomized binary file, over a mmWave network channel, with its conditions to be emulated using the generated pair of per-timeslot losses and RTT vectors (for each MCS scenario, a pair of vectors was collected, see Fig. 5). The throughput and the in-order delivery delay metrics are collected from the measurements of per-packet simulation result vectors. The defined scenario consists of a file divided into 100 datagrams of 1000 bytes each. With respect to the RLNC encoder and the decoder, the generation/maximum window

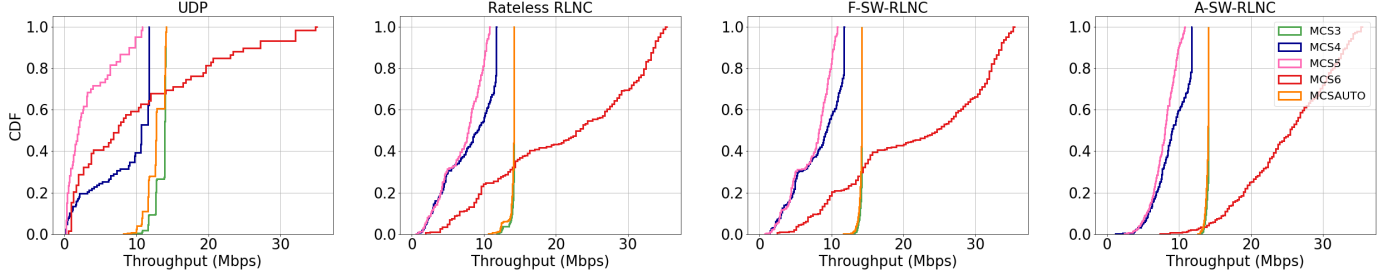


Fig. 6: Normalized throughput results.

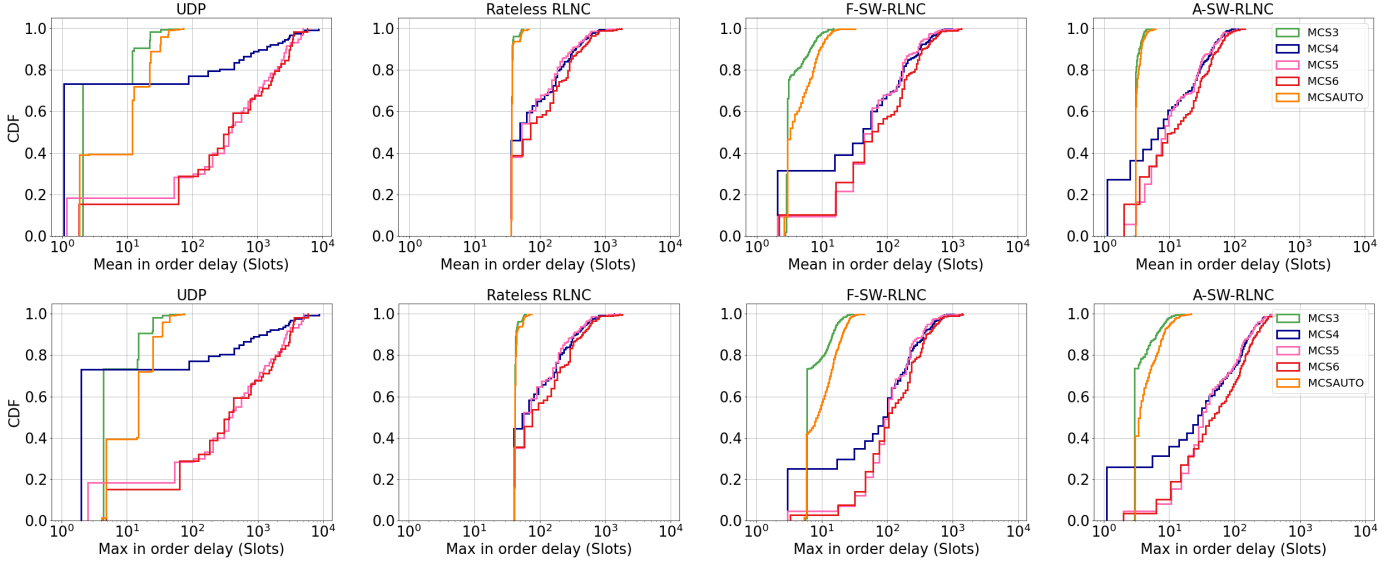


Fig. 7: Mean and maximum in-order delay results.

size is set to 20 packets.

C. Modulation Coding Schemes vs Packet Loss

Figure 5 presents the RTT and lost packets for individual MCS modes obtained in the experimental mmWave testbed. As expected, packet loss is more prominent for higher MCS values, due to the use of the combination of less reliable modulation (QPSK/BPSK) with a higher FEC rate. Furthermore, the data shows that, locking MCS3 for both directions and setting the antenna modules to select the MCS level accordingly to channel state yields similar behaviors when partially obstructed by the metallic plate. A high RTT variance for levels MCS4 through MCS6 is present, leading to several issues in the upper layers, and at the same time influencing the efficiency of RLNC-based schemes, by the late reaction time to successfully signal the decoding completion.

D. RLNC over mmWave

Setting the above channel behavior vectors for RTT and packet loss, as well as the aforementioned parameters, as inputs of the algorithm simulator shows significant improvement on in-order delivery delay and normalized data throughput.²

²The results of this section consider the transmission interval for each timeslot between datagrams in the transport layer, and the MCS coding rate on the PHY layer.

1) *Throughput*: The normalized throughput curves in Fig. 6 show that the robustness of the A-SW-RLNC over the mmWave network link pertains a higher overall throughput across all MCS modes, despite the high RTT variance. Higher MCS levels obtain higher throughput gains, as per time-slot feedback packets permit state synchronization between the encoder and the decoder for each sent packet, culminating in 100% delivery success for each connection, i.e., experience. For MCS3 level and automatic mode, A-SW-RLNC tops other coding solutions only slightly ahead, stabilizing the cumulative density function (CDF) curve, i.e. stabilizing eventual spikes in worsened link conditions. Table II shows that, for the MCS Auto mode, there is no improvement on the first percentile between the Rateless code with a sliding window implementation over A-SW-RLNC, meaning that for low error rates, A-SW-RLNC shows no significant throughput penalty. For higher levels of MCS, there is a significant improvement on 1% bounds with A-SW-RLNC.

2) *Mean In-Order Delivery Delay*: Simulation results show that the A-SW-RLNC solution performs exceptionally well regarding in-order delivery delays in comparison with the simpler rateless solutions over the mmWave channel vector, as illustrated in Figure 7. Regarding the mean in-order delay, with MCS3 and automatic MCS modes, CDF curves show that the simple UDP transmission gets better results than the rateless RLNC standard algorithm. Packets encoded

TABLE II: Statistics for simulation results of tested algorithms from MCS3 to MCS6, and Auto modes. For a time slot of $450\mu\text{s}$, the scheme that achieves **LLC** and **URLLC** are marked.

Mode	Algorithm	Throughput (Mbps)				Mean In-Order Delay (slots)				Max In-Order Delay (slots)			
		Mean	Stdev	$P_1\%$	$P_{99\%}$	Mean	Stdev	$P_1\%$	$P_{99\%}$	Mean	Stdev	$P_1\%$	$P_{99\%}$
MCS3	UDP transmission	13.57	0.86	10.80	14.17	6.29	7.74	2.16	32.95	8.95	7.74	4.73	35.67
	Rateless	14.08	0.35	12.36	14.22	37.67	2.64	36.50	51.62	42.52	2.84	40.80	40.80
	F-SW-RLNC	14.15	0.18	13.37	14.22	3.85	1.97	2.80	12.11	8.13	4.24	5.76	24.21
	A-SW-RLNC	14.00	0.19	13.30	14.08	3.11	0.29	2.00	4.31	3.86	1.95	2.00	11.38
	A-SW-RLNC FF95%	14.00	0.51	13.45	14.08	3.04	0.15	2.00	3.61	3.72	1.71	2.00	10.83
	A-SW-RLNC FF99%	14.00	0.18	13.29	14.08	3.09	0.23	2.00	4.08	3.91	1.96	2.00	11.78
MCS4	UDP transmission	8.62	4.27	0.23	11.85	425.44	1180.34	1.06	5106.57	427.41	1180.38	2.00	5108.70
	Rateless	8.10	3.59	1.40	11.85	140.53	180.12	36.02	765.62	148.18	181.56	40.01	779.55
	F-SW-RLNC	8.33	3.39	1.59	11.85	114.29	163.71	2.06	681.71	145.74	175.30	2.00	734.11
	A-SW-RLNC	9.11	2.36	3.87	11.85	16.66	20.04	2.00	80.23	63.86	77.37	2.00	324.84
	A-SW-RLNC FF95%	9.20	2.23	3.94	11.85	9.85	10.81	2.00	47.56	53.15	64.10	2.00	266.22
	A-SW-RLNC FF99%	9.16	2.23	4.26	11.85	12.38	13.71	2.00	61.89	54.54	62.97	2.00	271.85
MCS5	UDP transmission	3.37	3.32	0.22	10.86	1004.99	1300.52	1.57	4980.49	1007.07	1300.57	3.74	4982.72
	Rateless	7.07	2.87	1.23	10.85	137.53	178.17	36.41	805.66	146.27	179.22	40.35	820.97
	F-SW-RLNC	7.40	2.74	1.57	10.94	115.35	149.07	2.71	635.49	156.07	154.91	5.69	688.98
	A-SW-RLNC	7.93	1.72	3.68	10.83	17.72	19.50	2.17	98.44	68.36	73.52	3.16	328.87
	A-SW-RLNC FF95%	8.10	1.68	3.54	10.80	10.04	10.29	2.14	47.87	56.88	64.30	2.71	294.74
	A-SW-RLNC FF99%	7.97	1.66	3.72	10.87	13.16	12.37	2.08	59.35	59.78	57.82	2.94	281.64
MCS6	UDP transmission	10.64	9.78	0.80	33.52	1029.80	1299.62	7.20	4601.51	1031.76	1299.59	9.38	4604.08
	Rateless	21.39	10.36	3.45	35.13	177.93	228.41	36.81	999.80	186.20	229.38	41.26	1009.81
	F-SW-RLNC	22.04	10.07	3.97	35.52	154.31	192.85	3.05	848.23	193.42	199.65	7.85	899.50
	A-SW-RLNC	25.17	6.36	11.01	35.56	22.28	23.63	2.00	100.38	87.16	88.85	2.00	405.18
	A-SW-RLNC FF95%	25.70	6.12	10.81	35.14	11.77	11.47	2.00	49.37	70.03	71.46	2.00	294.64
	A-SW-RLNC FF99%	25.57	5.95	12.13	35.56	15.72	14.53	2.00	59.23	72.28	66.27	2.00	267.64
Auto	UDP transmission	12.82	1.21	9.99	14.15	12.96	11.63	2.18	43.20	15.60	11.63	4.70	45.82
	Rateless	13.98	0.50	11.86	14.22	38.31	4.03	36.56	55.08	43.27	4.20	40.90	61.43
	F-SW-RLNC	14.08	0.27	13.03	14.22	5.15	3.29	2.83	15.43	11.25	6.48	5.70	29.90
	A-SW-RLNC	13.92	0.24	12.98	14.08	3.22	0.42	2.00	4.90	4.78	2.71	2.00	14.85
	A-SW-RLNC FF95%	13.93	0.53	13.11	14.08	3.08	0.18	2.00	3.76	4.46	2.49	2.00	14.80
	A-SW-RLNC FF99%	13.90	0.54	13.04	14.08	3.19	0.34	2.00	4.57	4.97	2.78	2.00	14.25

in a block/generation are decoded only if the decoder receives a number of codes equal to the generational size (Section III-A), limiting the minimum theoretical achievable delay of the generational size for each packet. The sliding window implementation removes this limitation, and achieves better results for the upper quartile and above with an order of two. A-SW-RLNC triples this prior improvement on the 99th percentile over the former one, sliding-window RLNC scheme, as per values in Table II. This gain is justified with the tracking of channel erasures and the dynamic FEC transmission slot definition in relation to the channel rate (Section III-B). For higher level MCS modes, the sharp increase in the channel erasure rate makes simple UDP file transfer to be unusable, as file retransmission probability is substantial, therefore increasing packet in-order delivery delay. The RLNC block implementation mitigates these losses via naive code redundancy, improving the high in-order delay of a UDP transmission. From the CDF graphs, gains start for the upper steps of the 20th percentile, peaking on a 9:1 improvement ratio for the 70th percentile. Similarly to the lower MCS level behavior, although not as prominent, the rateless *slide* RLNC implementation gets a slight performance improvement with respect to the 99% guarantees, as shown in Table II - an increase of 17.8%. A-SW-RLNC gets highly ahead in this regard - the adaptive and dynamic component, as previously mentioned, is now evident from the 99% guarantee threshold, outperforming the former algorithm with a factor of 8.4. The obtained guarantee improvement is approximately

10 times over the rateless RLNC coding solution.

3) *Maximum In-Order Delivery Delay*: With respect to the maximum in-order delivery delay, it is shown in Figure 7 that the rateless RLNC algorithm does not differ much from the previous analyzed mean delay values, showing that its bounds are quite close. Although penalized by its generational size at low MCS values (as MCS3/MCS Auto), as shown in Table II, the statistical values for the maximum delay get a significant improvement with a factor of 4.5 times for the 99% guarantees, and 5.5 times for the mean values at MCS6. Similarly to the mean value for the in-order delivery delay, the sliding-window rateless RLNC gets a slight increase in the results. A-SW-RLNC gets an improvement with a ratio of 2 to 2.5 across all percentile bounds over the former approach, for the MCS Auto mode. Compared to the baseline UDP transmission results, however, the adaptive and causal algorithm at the higher MCS tested, MCS6, for the 99% maximum delay, results in much lower guarantees, with a decrease over 11 times.

4) *LLC and URLLC performance*: Regarding the support of low latency and ultra-reliable scenarios in the mmWave IAB, Table II highlights each scheme capable to achieve **LLC** and **URLLC** applications. For **LLC** applications, we consider a mean in-order delay below 10ms (22 slots). For **URLLC** applications (only $P_{99\%}$), a max in-order delay below 10ms (22 slots) was used as the threshold. As presented in Table II, only the A-SW-RLNC can support **URLLC** applications, by obtaining a max in-order delay below 10 ms for $P_{99\%}$. In such lossy links, transport protocols like UDP cannot be

used in URLLC scenarios, as well as the rateless and the F-SE-RLNC schemes. When addressing LLC applications, the A-SW-RLNC scheme presents a huge improvement, when compared with all the other schemes, and also with the dynamic approach used by lower layers (auto). The A-SW-RLNC scheme is capable to achieve a delay below 10ms in all the MCSs evaluated, allowing the increase of the network bandwidth by using a higher MCS. As presented, low-layer techniques are very conservative and do not allow to take the full benefits of the mmWave link capacity.

V. CONCLUSIONS AND FUTURE VISIONS

In this work, we proposed a significant enhancement on the mmWave performance by incorporating network coding algorithms to stabilize the high-frequency communication sensitivity. In particular, we showed that using A-SW-RLNC, it is possible to obtain ultra-reliable high bandwidth while reducing by up to an order of two the mean in-order delay. Our results demonstrate that the communication protocols can notably take benefit from relaxing the PHY and MAC layer error control mechanisms, and delegating the task to the upper layers using the proposed network coding solution. In fact, the retransmissions that occur due to MAC error control mechanisms are effectively not needed once the network coding solution and FEC mechanisms are utilized.

As for future work, we plan to use the gain of multipath (MP) network coding communication through splitting the mmWave band into several sub-bands. For this end, we will extend the proposed single-path (SP) solution to several frequency links via an effective MP coded communication. To use the proposed solution over highly-meshed backhaul of novel communication networks, we plan to incorporate software-defined controllers for collecting information that can enhance the communication performance over meshed mmWave communication [27]. Last but not the least, we plan to exploit the recent trend in estimation of error patterns using deep-learning solutions to further improve our adaptive solutions over mmWave networks [28].

VI. ACKNOWLEDGMENTS

This work is supported by the European Regional Development Fund (FEDER), through the Regional Operational Programme of Centre (CENTRO 2020) of the Portugal 2020 framework and FCT under the MIT Portugal Program [Project SNOB-5G with Nr. 045929(CENTRO-01-0247-FEDER-045929)]

REFERENCES

- [1] Y. Xu, G. Gui, H. Gacanin, and F. Adachi, "A survey on resource allocation for 5g heterogeneous networks: Current research, future trends, and challenges," *IEEE Communications Surveys Tutorials*, vol. 23, no. 2, pp. 668–695, 2021.
- [2] T. Nitsche, C. Cordeiro, A. B. Flores, E. W. Knightly, E. Perahia, and J. C. Widmer, "IEEE 802.11 ad: directional 60 GHz communication for multi-Gigabit-per-second Wi-Fi," *IEEE Communications Magazine*, vol. 52, no. 12, pp. 132–141, 2014.
- [3] X. Wang, L. Kong, F. Kong, F. Qiu, M. Xia, S. Arnon, and G. Chen, "Millimeter wave communication: A comprehensive survey," *IEEE Communications Surveys and Tutorials*, vol. 20, no. 3, pp. 1616–1653, 2018.
- [4] Y. Ren, W. Yang, X. Zhou, H. Chen, and B. Liu, "A survey on TCP over mmWave," *Computer Communications*, vol. 171, no. February, pp. 80–88, 2021. [Online]. Available: <https://doi.org/10.1016/j.comcom.2021.01.032>
- [5] A. Shokrollahi, "Raptor codes," *IEEE/ACM Transactions on Networking (TON)*, vol. 14, no. SI, pp. 2551–2567, 2006.
- [6] M. Luby, "LT codes," in *Proc. IEEE Symp. Found. Computer Science*. IEEE, 2002, pp. 271–280.
- [7] (2021, December) Bitriple, qualcomm technologies and verizon work together to enable the first 8k hdr smartphone video call over 5g. [Online]. Available: <https://6park.news/hawaii/bitriple-qualcomm-technologies-and-verizon-work-together-to-enable-the-first-8k-hdr-smartphone-video-call-over-5g-news.html>
- [8] J. Cloud, D. Leith, and M. Médard, "A coded generalization of selective repeat ARQ," in *2015 IEEE Conf. Computer Commun*, 2015, pp. 2155–2163.
- [9] G. Joshi, Y. Kochman, and G. W. Wornell, "On playback delay in streaming communication," in *Proc. IEEE Int. Sym. Inf. Theory*, 2012, pp. 2856–2860.
- [10] —, "The effect of block-wise feedback on the throughput-delay trade-off in streaming," in *Proc. IEEE Conf. Computer Commun. Wkshps*, 2014, pp. 227–232.
- [11] V. Cerf and R. Kahn, "A protocol for packet network intercommunication," *IEEE Transactions on communications*, vol. 22, no. 5, pp. 637–648, 1974.
- [12] V. Cerf, Y. Dalal, and C. Sunshine, "Specification of internet transmission control program," RFC 675, December, Tech. Rep., 1974.
- [13] T. Ho, M. Médard, R. Koetter, D. R. Karger, M. Effros, J. Shi, and B. Leong, "A random linear network coding approach to multicast," *IEEE Trans. Inf. Theory*, vol. 52, no. 10, pp. 4413–4430, 2006.
- [14] D. S. Lun, M. Médard, R. Koetter, and M. Effros, "On coding for reliable communication over packet networks," *Physical Commun.*, vol. 1, pp. 3–20, Mar. 2008.
- [15] L. Yang, Y. E. Sagduyu, J. Zhang, and J. H. Li, "Deadline-aware scheduling with adaptive network coding for real-time traffic," *IEEE/ACM Transactions on Networking*, vol. 23, no. 5, pp. 1430–1443, 2014.
- [16] "Aveiro Smart-City Open Lab." [Online]. Available: <https://aveiro-living-lab.it.pt/>
- [17] A. Cohen, D. Malak, V. B. Bracha, and M. Médard, "Adaptive causal network coding with feedback," *IEEE Transactions on Communications*, vol. 68, no. 7, pp. 4325–4341, 2020.
- [18] A. Cohen, G. Thiran, V. B. Bracha, and M. Médard, "Adaptive causal network coding with feedback for multipath multi-hop communications," *IEEE Transactions on Communications*, vol. 69, no. 2, pp. 766–785, 2020.
- [19] "Ieee standard for information technology–telecommunications and information exchange between systems–local and metropolitan area networks–specific requirements–part 11: Wireless lan medium access control (mac) and physical layer (phy) specifications amendment 3: Enhancements for very high throughput in the 60 ghz band," *IEEE Std 802.11ad-2012 (Amendment to IEEE Std 802.11-2012, as amended by IEEE Std 802.11ae-2012 and IEEE Std 802.11aa-2012)*, pp. 1–628, 2012.
- [20] "Metnet 60g unlicensed mmwave mesh datasheet - ccsl.com," 02 2020. [Online]. Available: <https://www.ccsl.com/v1/uploads/files/Metnet-60G-Mesh-datasheet.pdf>
- [21] A. Richardson and J. Brady, "Using self-organizing mmWave to deliver 5G services." [Online]. Available: https://www.bcba.ca/application/files/5515/5812/9724/CCS_Metnet__Broadnet.pdf
- [22] B. Schultz, "802.11 ad - wlan at 60 ghz - a technology introduction," *Rohde & Schwarz*, 2013.
- [23] M. Dahhani, G. Jakllari, and A. L. Beylot, "Association and Reliability in 802.11ad Networks: An Experimental Study," *Proceedings - Conference on Local Computer Networks, LCN*, vol. 2019-October, pp. 398–405, 2019.
- [24] Y. Shi, Y. E. Sagduyu, J. Zhang, and J. H. Li, "Adaptive coding optimization in wireless networks: Design and implementation aspects," *IEEE Transactions on Wireless Communications*, vol. 14, no. 10, pp. 5672–5680, 2015.
- [25] J. Babiary, R. M. Krzanowski, K. Hedayat, K. Yum, and A. Morton, "A Two-Way Active Measurement Protocol (TWAMP)," RFC 5357, Oct. 2008. [Online]. Available: <https://www.rfc-editor.org/info/rfc5357>
- [26] Steinwurf, "Kodo-python," <https://github.com/steinwurf/kodo-python>, 2022.
- [27] A. Cohen, H. Esfahanizadeh, B. Sousa, J. P. Vilela, M. Luís, D. Raposo, F. Michel, S. Sargento, and M. Médard, "Bringing Network Coding into

- SDN: Architectural Study for Meshed Heterogeneous Communications,” *IEEE Communications Magazine*, vol. 59, no. 4, pp. 37–43, 2021.
- [28] A. Cohen, A. Solomon, and N. Shlezinger, “Deepnp: Deep learning-based noise prediction for ultra-reliable low-latency communications,” *arXiv preprint arXiv:2110.15328*, 2021.